

Biaxial dielectric properties of phenyl ester ferroelectric liquid crystal mixture

Y. B. KIM, I. K. HUR, J. W. CHOI

Liquid Crystal Research Center, Department of Chemistry, College of Sciences, Kon-Kuk University, 1, Hwayangdong, Kwangjinku, Seoul, 133-701, South Korea
E-mail: yongkim@kkucc.konkuk.ac.kr

M. BUIVYDAS, F. GOUDA, S. T. LAGERWALL

Physics Department, Chalmers University of Technology, S-41296 Gothenberg, Sweden

Dielectric and electro-optic properties of phenyl ester FLC mixture have been studied in detail. Dielectric relaxation spectroscopy was used to study the molecular dynamics and dipolar ordering. In the SmA* phase, this is accompanied by a sharp increase in the dielectric strength $\Delta\epsilon_s$ on approaching T_c . At such high frequency (2 MHz) $\Delta\epsilon$ is usually negative in the SmC* and SmA* phase. In the N* phase, at lower frequencies, $\Delta\epsilon$ had a weakly positive value. In the SmC* phase, $\delta\epsilon$ is positive and its maximum value is less than 0.1. The dielectric biaxiality is discussed as an order parameter of the tilted smectic phase. It is verified that if the tilt angle increases according to $\theta \propto (T_c - T)^\beta$, the biaxiality increases according to $\delta\epsilon \propto (T_c - T)^{2\beta}$. A critical exponent for θ and $\delta\epsilon$ are 0.27 and 0.54, respectively. The rotational viscosity γ_θ for soft mode is of 10 Nsec/m² in the SmA* phase. The activation energy for the rotational dynamics of Goldstone mode is estimated to be 1.4 eV from an Arrhenius plot. Optical response time is of about 50 μ s at room temperature in SmC* phase, and is on the order of 10 μ s in the N* phase and almost independent of the applied field.

© 2000 Kluwer Academic Publishers

1. Introduction

Since the discovery of ferroelectric liquid crystals (FLCs) by Meyer *et al.* [1] and the invention of the surface-stabilized ferroelectric liquid crystal displays (SSFLCD) by Clark and Lagerwall [2], FLCs have attracted a great interest both from the theoretical research and application to displays. Usually, for practical application, FLCs mixture shows a fast response time on the order of microseconds. The response time depends on the magnitude of the spontaneous polarization and rotational viscosity of the FLCs mixtures. The chirality of the optical active group of ferroelectric liquid crystal molecule is one of important factors to determine a polarization in SmC* phases. The strong chirality gives rise to short pitch values [3]. This strong chirality and the presence of a -COO- functional group near the chiral center carbon gives a fairly large electroclinic effect in TGBA phase [4].

The tilt angle is an important parameter describing the molecular orientations in the SmC* phase and influencing the characteristics of FLC devices. The tilt angle is known to influence the spontaneous polarization and the response time [5, 6]. Also, the rotational viscosity is an important parameter for understanding the dynamics of ferroelectric electro-optic switching. It is only very recently that progress has been made in developing accurate and reasonably simple methods for viscosity determinations. Such methods include pyroelectric techniques [7], electro-optic methods [8] and

measurements of the polarization current using square wave or triangular wave driving voltage [9].

The dielectric biaxiality is a recently recognized parameter with considerable influence on the performance of various FLC devices [10]. The importance of dielectric torque on the switching behavior of FLC is manifested by the minimum usually observed [11] in the high field regime of the electro-optic switching time. It is the magnitude rather than the anisotropy that is crucial to the existence of this minimum. The dielectric behavior of the SmC* and SmA* phase and its dependence on temperature, frequency and electric bias field [12, 13] has been studied by several groups during the last few years. The main outcome of these studies has been the characterization of the dielectric properties of the Goldstone mode in the SmC* phase and the soft mode in the SmA* phase.

Dielectric spectroscopy is a powerful method to study the molecular dynamics of collective and non-collective molecular origin. In the SmC* phase, the dielectric spectrum exhibits two absorption peaks attributed to the soft mode due to the tilt fluctuations, and the Goldstone mode due to the phase fluctuations. In the SmA* phase, because of the disappearance of the tilt, the dielectric spectrum exhibits only one absorption peak due to the soft mode. These two processes are usually observed in the bookshelf geometry, i.e. with the smectic layers essentially perpendicular to the glass plates. In the homeotropic orientation (the

smectic layers are parallel to the glass plates), however, the dielectric spectrum exhibits an absorption peak due to the molecular reorientation around the short axis of the molecules.

In the present work, the dielectric strength and the relaxation frequency of different molecular processes of a ferroelectric liquid crystal mixture is discussed. These measurements enabled us to determine the rotational viscosity of the soft mode and Goldstone mode, γ_θ and γ_φ in the SmA* and SmC*, respectively.

2. Experimental

The ferroelectric liquid crystal mixture (KU-1010) was prepared with one non-chiral and two ferroelectric liquid crystal compounds as exhibited in Fig. 1. Compound I was synthesized with 4-hydroxybiphenyl 4'-alkoxybenzoate and (2S, 3S)-2-chloro-3-methylpentanoic acid by esterification reaction [14]. The chemical structures of the final compounds were checked by a combination of nuclear magnetic resonance spectroscopy (Hitach 60 MHz spectrometer), Infrared spectroscopy (BIO-RAD FTS-60 Spectrometer) and mass spectrometry (Hewlett Packard 6180). The molecular formulae and phase sequence are shown in Fig. 1. The transition temperature and the phase sequence that "Crystal -10°C SmX* 22°C SmC* 53°C SmA* 75°C N* 82°C Isotropic" have been determined by differential scanning calorimeter (DSC: Perkin-Elmer7) and polarizing microscope (Zeiss photomicroscope II Pol) in conjunction with a Mettler FP52 hot stage.

We used the test cells of conventional sandwich type, consisting of two ITO glass plates, separated at a constant distance (2 μm) by evaporated SiO spacers. The electrode sides of the ITO glass plates were coated with an insulating protection layer of SiO about 1000 Å thick. The liquid crystal is introduced into the cell by means of capillary force. A planer textures in smectic C* phase is obtained by a gentle shearing of the cell while applying a high electric field across it.

The cell was placed in a Mettler FP52 hot stage with the temperature controlled within 0.1°C accuracy. The investigation of electro-optical characteristics was carried out using a Zeiss photomicroscope II Pol. and the response was detected and monitored by photodiode and an oscilloscope, respectively.

The spontaneous polarizability (P_s) was measured by the AC Bridge method. The tilt angle (θ) was

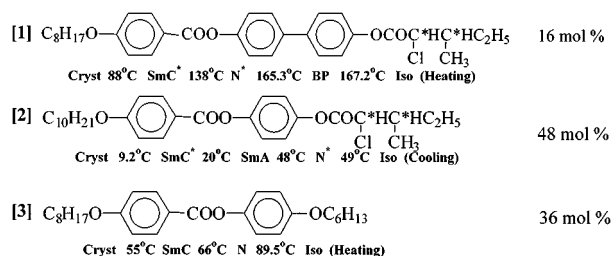


Figure 1 Components of ferroelectric liquid crystal mixture KU-1010.

microscopically observed by a field reversal method. The response time (10–90) was defined as that time when 10–90% of the transmission value was detected by a photodiode. The rotational viscosity γ_φ for a cone motion in the SmC* phase was calculated using the well known empirical relation: $\gamma_\varphi = (1/1.8)t_{10-90}P_sE$, where E is the applied switching field [15].

The dielectric measurements were carried out in the frequency range 10 Hz to 10 MHz using a HP 4192 LF impedance analyzer. In order to probe the principal components of the dielectric tensor in different phases, the dielectric measurements were made on different measurement geometry. The first set of measurement is carried out on a 2 μm -thick sample with a homeotropic molecular orientation achieved by strong shearing of the glass plates. The measured dielectric permittivity in this geometry is denoted ϵ_{hom} . The second set of measurement is carried out on an 18 μm -thick sample, and the planar orientation was achieved by applying an ac electric field. The measured dielectric permittivity in this geometry is denoted ϵ_{plan} . In the SmC* phase, at sufficiently high frequency, a bias electric field was applied to unwind the helical structure, it is denoted ϵ_{unw} . It is worth pointing out that in the N* phase, measurements are made with the helical axis parallel (ϵ_{hom}) and perpendicular (ϵ_{plan}) to the glass plates. In the first case, $\epsilon_{\text{hom}} = (\epsilon_{\parallel} + \epsilon_{\perp})/2$. However, when the helical axis is perpendicular to the glass plates, the measured $\epsilon = \epsilon_{\perp}$. The dielectric contribution of the soft mode and Goldstone mode has been measured in the planar orientation. In order to observe the soft mode in the SmC* phase, a bias electric field of 25 volt/50 μm (quenching the Goldstone mode) was applied. It is convenient in this context, to comment on the experimental difficulties encountered in measuring the soft mode in the SmC* phase. As mentioned earlier, in the tilted phase, there are two director modes: the Goldstone mode and soft mode. The dielectric strength of the Goldstone mode, except in the very vicinity of T_C , is larger than that of the soft mode by orders of magnitude. Thus, it is non-trivial to extract the soft mode dielectric response in the SmC* phase. One way to overcome this problem is to apply a bias electric field over the sample in order to unwind the helix and lock the direction of polarization in space, thus suppressing the Goldstone mode dielectric response. This enabled us to study the soft mode response in a broad temperature interval of 23°C below T_C , which otherwise could hardly be observed for more than a few tenths of a degree away from the transition into the SmC* phase.

A point worth to emphasize is that the measured soft mode dielectric response in the SmC* phase certainly is affected by the bias electric field [16], however, the perturbation is found to be pronounced in the vicinity of T_C but negligibly small already at about 1°C below the SmA* to SmC* transition point. Thus, except in a temperature interval of one degree below T_C , the measured values of ϵ_s and f_s in the SmC* phase are accurate and field independent.

In order to extract the correct values of the dielectric strength, $\Delta\epsilon$, relaxation frequency, f_R , and distribution parameter, α , the following equation has been

fitted to measured frequency dependence of dielectric absorption ε''

$$\varepsilon'' = \frac{\sigma}{2\pi\varepsilon_0} \left(\frac{1}{f^n} \right) + \text{Im} \left(\varepsilon(\infty) + \frac{\Delta\varepsilon}{1 + \left(j \frac{f}{f_R} \right)^{1-\alpha}} \right) + a(R, C)f^m \quad (1)$$

where the first term represents the contribution from the freely moving charges (ε_0 is the vacuum permittivity) and the third terms arises from the ITO resistive layer. The second term is the imaginary part of the Cole-Cole equation.

In the smectic A phase, the dielectric anisotropy is simply defined as $\Delta\varepsilon = \varepsilon_{\parallel} - \varepsilon_{\perp}$, which no longer makes sense in the SmC* phase. It has been customary to speak of $\Delta\varepsilon = \varepsilon_3 - \varepsilon_1$ as the dielectric anisotropy in this phase, and of the splitting $\delta\varepsilon = \varepsilon_2 - \varepsilon_1$ as the dielectric biaxiality. The tilt angle θ of both substances was measured by the conventional method based on the angular reading of the optic axis on the SmC* cone corresponding to the high field saturated values of the switching positions. In order to calculate the perceptivities ε_1 , ε_2 and ε_3 , the following equations were used [17].

$$\varepsilon_1 = \frac{1}{1 - 2 \sin^2 \theta} \left[\frac{\cos^2 \theta}{\cos^2 \delta} (2\varepsilon_{\text{helix}} - \varepsilon_{\text{unw}} - \varepsilon_{\text{hom}} \sin^2 \delta) - \varepsilon_{\text{hom}} \sin^2 \theta \right] \quad (2)$$

$$\varepsilon_2 = \frac{1}{\cos^2 \delta} (\varepsilon_{\text{unw}} - \varepsilon_{\text{hom}} \sin^2 \delta) \quad (3)$$

$$\varepsilon_3 = \frac{-1}{1 - 2 \sin^2 \theta} \left[\frac{\cos^2 \theta}{\cos^2 \delta} (2\varepsilon_{\text{helix}} - \varepsilon_{\text{unw}} - \varepsilon_{\text{hom}} \sin^2 \delta) - \varepsilon_{\text{hom}} \cos^2 \theta \right] \quad (4)$$

where $\delta = 0.8\theta$. This is a reasonable approximation that is valid for a large number of substances and first deduced from X-ray studies performed by Ricker *et al.* [18]. Although δ/θ does depend on the temperature to some extent, the ε values do not depend very critically on this ratio.

3. Results and discussion

3.1. Polarization and tilt angle

The components of the KU-1010 mixture are phenyl esters liquid crystal compounds of similar structure to shown in Fig. 1. Our mixture exhibited the phase sequence that Cry -10.7°C SmX* 22.6°C SmC* 53.2°C SmA* 75.1°C N* 82.4°C Iso, which is determined by optical polarizing microscopy and differential scanning calorimeter. The optically active group of the fer-

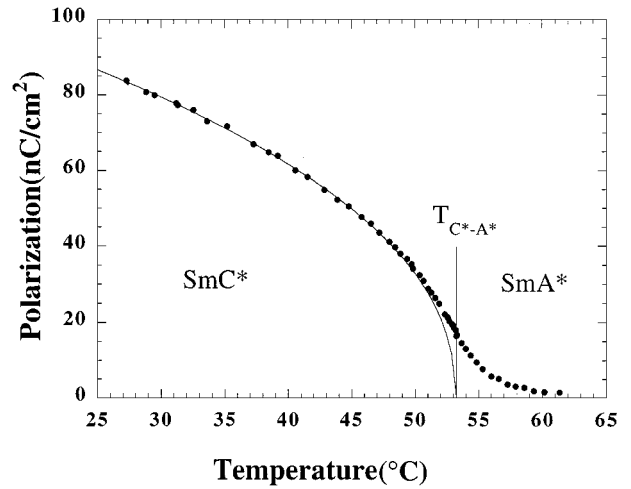


Figure 2 Temperature dependence of the spontaneous polarization.

roelectric liquid crystals has two chiral centers. The spontaneous polarization (P_s) as a function of temperature are exhibited in Fig. 2. The spontaneous polarization increased with decreasing temperature below the SmC*-SmA* transition. A fairly large P_s of 83.2 nC/cm^2 was observed at 28° in the SmC* phase. A typical temperature dependence of the polarization, and the pretransition are observed in the vicinity of the SmC*-SmA* transition point as shown in Fig. 2. We made a least square adjustment of our data on a law of the form: $P_s(T) \propto (T_c - T)^\beta$, where $P_s(T)$ is the polarization at temperature T , T_c is the SmC*-SmA* phase transition temperature, β is a critical exponent, which may be expected to vary between 0.5 and 0.25. We got $\beta = 0.45$ and $T_c = 53.2^\circ\text{C}$ as adjustment parameters from the best fit that is exhibited as a solid line in Fig. 2. It is well agreed with the other investigations of various materials. The induced polarization is observed in the SmA* phase at near the SmC*-SmA* phase transition, which was measured by means of a triangle-wave technique. It was obviously distinguished from the true polarization in the SmC* phase. This dependency is often observed for FLC compounds that exhibit a second order SmC*-SmA* phase transition. Our mixture is composed with the compounds bearing two chiral centers, which resulted in strong chirality. The strong chirality and the presence of a -COO- and -Cl functional groups near the chiral carbon induced a strong polarization and a helical structure in SmA* phase.

3.2. Dielectric relaxation spectroscopy

The temperature dependence of the dielectric strength and relaxation frequency measured in different phases is shown in the Figs 3 and 4, respectively. On both sides of the SmA* to SmC* transition, the relaxation frequency of the soft mode exhibits the expected slowing down behavior and the dielectric strength (Fig. 5) shows a diverging-like behavior when approaching the SmA*-SmC* transition temperature T_c . This temperature dependence is typical of a soft mode. It may be noted that the cut-off frequency at T_c is about 1 kHz. In the SmC* phase, the Goldstone mode dielectric response increases from 70 at T_c to 140 at 30 deep in

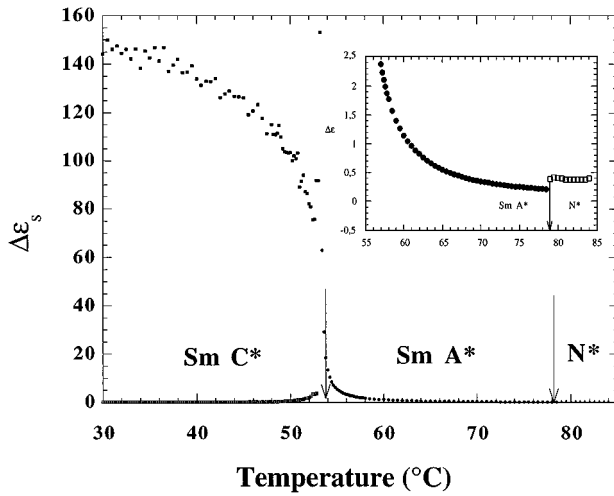


Figure 3 Temperature dependence of the dielectric strength in SmC*, SmA* and N* phases.

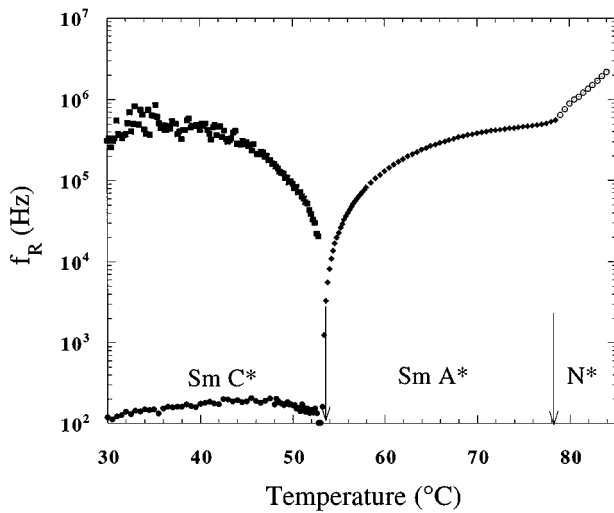


Figure 4 The dielectric strength of the soft mode versus temperature in SmC* and SmA* phases.

the SmC* phase. The dielectric contribution of the Goldstone mode, shown in Fig. 5, does not exhibit the broad maximum usually observed at about two degrees below the SmA* to SmC* transition. This could be attributed to the temperature dependence of the helical pitch that does not exhibit a maximum in the vicinity of T_C .

At the SmA* to N* phase transition (Fig. 3, sub-fig.), the dielectric strength exhibits a slight increase, and the relaxation frequency increases continuously, however, with a higher activation energy. The measured permittivity in the N* phase has a contribution from ϵ_{\parallel} and ϵ_{\perp} . The dynamics of these two components is connected with the molecular reorientation around the short and long axis of molecules, respectively. The characteristic frequency of these two processes is usually observed at the low MHz and GHz regimes of dielectric spectrum, respectively [19]. Thus, the process observed in our case can be attributed to the molecular reorientation around the short axis of the molecule. A mechanism that differs from the soft mode by the fact the soft mode is a *collective* tilt fluctuation. However, both mechanisms are connected with the reorientation around the short

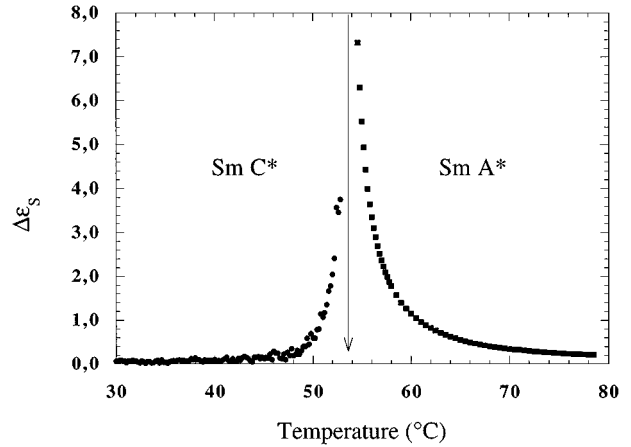


Figure 5 Temperature dependence of the relaxation frequencies of the Goldstone mode and soft mode responses in SmC*, SmA* and N* phases.

axis. This “common” aspect in their dynamics may explain the “smooth” temperature dependence of the relaxation frequency at the SmA* to N* transition.

The rotational viscosity of the soft mode γ_{θ} and the Goldstone mode γ_{φ} have been determined using the equations

$$\gamma_{\theta} = \frac{\epsilon_0 \epsilon^2(\infty) C^2}{2\pi} \left(\frac{1}{\Delta \epsilon_S f_S} \right) \quad (5)$$

$$\gamma_{\varphi} = \frac{1}{4\pi \epsilon_0} \left(\frac{P_S}{\theta} \right)^2 \left(\frac{1}{\Delta \epsilon_G f_G} \right) \quad (6)$$

where the bilinear coefficient C was determined from the electric field dependence of the induced tilt angle θ_{ind} measured in the SmA* phase as shown Fig. 6.

$$\theta_{\text{ind}} = \frac{\epsilon_0 \epsilon(\infty) C}{\alpha(T - T_C)} E \quad (7)$$

The temperature dependence of the soft mode rotational viscosity γ_{θ} and the Goldstone mode rotational viscosity γ_{φ} are shown in Fig. 7. It is found that γ_{θ} in the SmA* phase is larger than γ_{φ} in the SmC* phase by a factor of two, and the difference increases to a factor

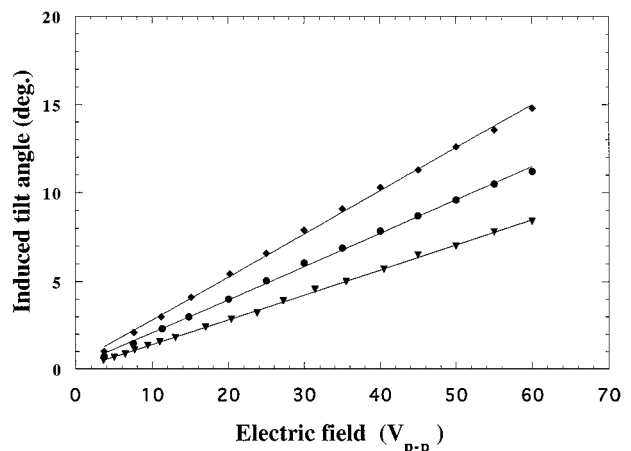


Figure 6 The induced tilt angle versus applied electric field in SmA* phase; \blacklozenge : 66.2°C, \bullet : 63.6°C, \blacktriangledown : 60.4°C.

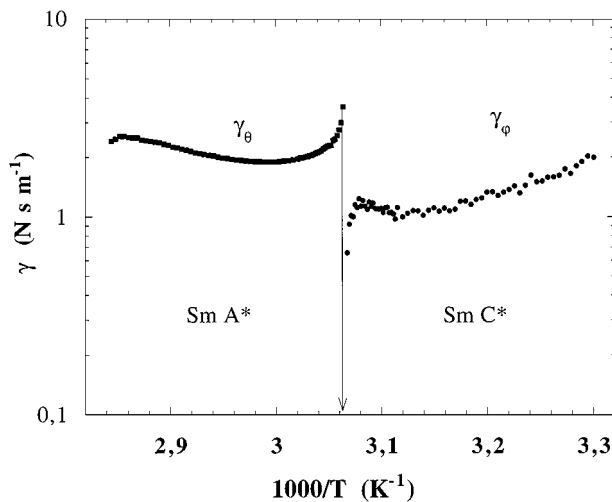


Figure 7 The soft mode and Goldstone mode rotational viscosities as the function of temperature.

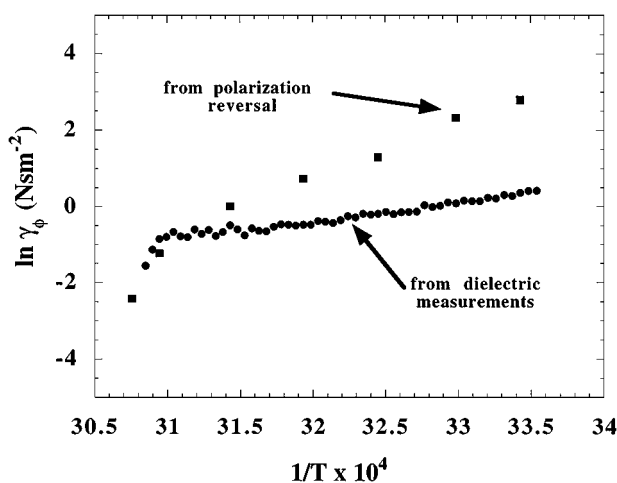


Figure 8 Comparative study of γ_ϕ rotational viscosity measured by polarization reversal technique and dielectric relaxation spectroscopy.

four when approaching the SmA* to SmC* transition. An Arrhenius plot of the apparent rotational viscosity γ'_ϕ by the polarization reversal method has been compared with the Goldstone mode rotational viscosity γ_ϕ obtained from the dielectric method. The results are shown in Fig. 8, The values of γ'_ϕ is a little larger than γ_ϕ at lower temperatures and the difference tends to be smaller at higher temperatures. Except the vicinity of the SmC*-SmA* phase transition, the results give a linear behaviour from which the activation energy is estimated to be 1.4 eV. The results are shown a good agreement between these two methods.

The temperature dependence of the dielectric permittivity measured in different measurement geometries are depicted in Fig. 9. The dielectric biaxiality in the SmC* phase has been determined using the method described by Gouda *et al.* [20]. Fig. 10 shows the temperature dependence of the dielectric anisotropy and dielectric biaxiality, At such a high frequency (2 MHz), $\Delta\epsilon$ is usually negative. In the N* phase, at lower frequencies, has a weakly positive value. In the SmC* phase, $\delta\epsilon$ is positive, and its maximum value is less than 0.1. This small value of $\delta\epsilon$ can be understood in terms of the molecular structure of the studied mixture. As re-

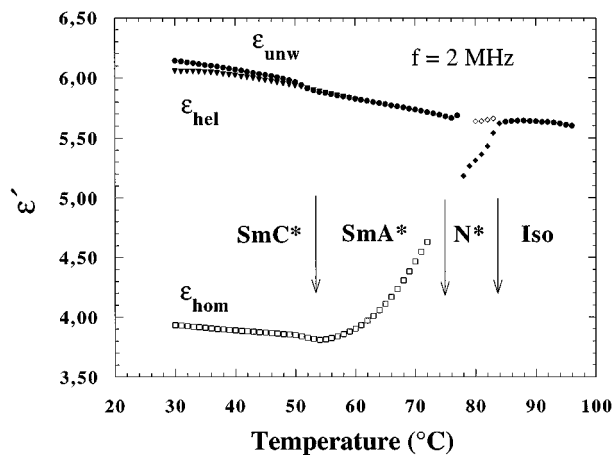


Figure 9 Temperature dependence of dielectric permittivity measured different geometries in the N* SmA* and SmC* phases.

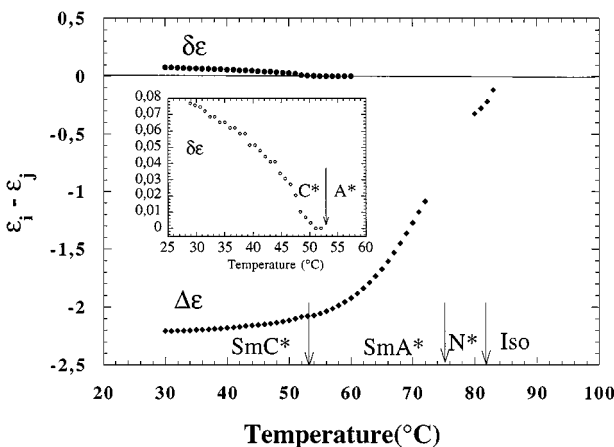


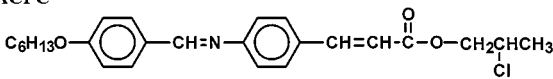
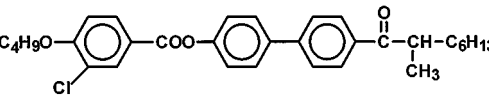
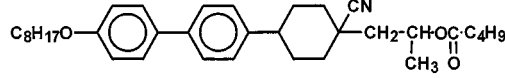
Figure 10 Temperature dependence of the dielectric anisotropy and dielectric biaxiality in different phases. the sub-figure shows, on a larger scale, the dielectric biaxiality in the SmC* phase.

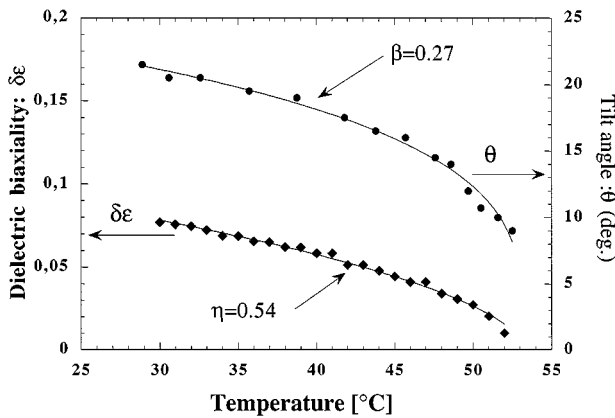
cently reported by Buivydas *et al.* [17], on the molecular level, it is noticed that attaching a strong polar group to the linking point of benzene (or cyclohexane ring) or any position of a ring and the alkyl chain results in the largest biaxiality $\delta\epsilon$ as illustrated in Table I.

The CD11 compound that has a slightly larger value of P_s (90.0 nC/cm²) possesses a large value of $\delta\epsilon$ (+4.75). This is due to the attribution of the CN group attached to the benzene ring, as can be seen from the formula in Table I. In case of KU-1010, none of the constituent molecules of our mixture has this polar structure, which has a relatively large P_s value (83.2n C/cm²), while at the same time, it has the lowest value (0.08) of dielectric biaxiality. It is clear that the large value of polarization originates from the Cl group attached to the asymmetric carbon. Therefore, $\delta\epsilon$ may be enhanced by attaching a strong polar group to one of the benzene rings directly connected to the alkyl chain.

In Fig. 11, we exhibit the power law fit of the temperature dependence of dielectric biaxiality and tilt angle in SmC* phase. The tilt angle decrease very slowly with increasing temperature over the temperature range of 28 to 45°C. Close to the SmC*-SmA* phase transition ($T_C = 53.2^\circ\text{C}$), the tilt angle decreases drastically. We got that the tilt angle is about 22° at 28°C and 8° at the SmC*-SmA* transition point. It is known that the

TABLE I Comparison of a values of the dielectric biaxiality $\delta\epsilon$, the dielectric anisotropy $\Delta\epsilon$ and polarizations P_s

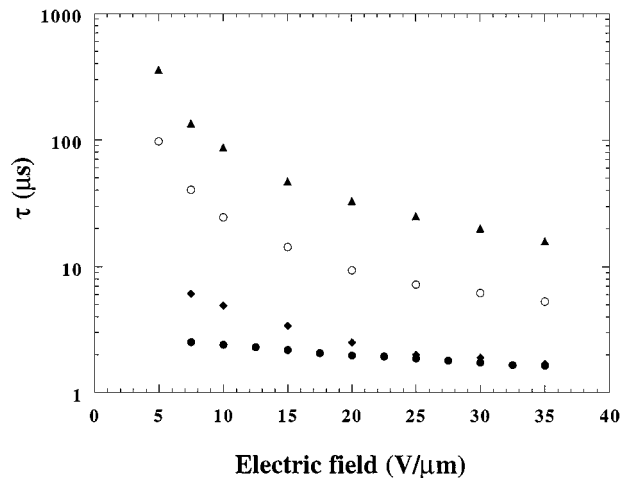
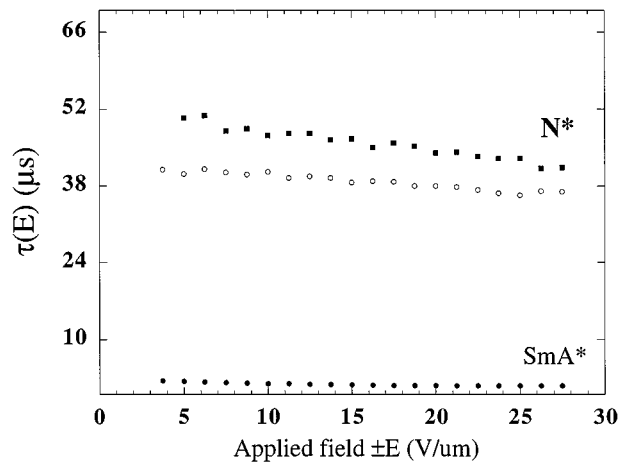
Chemical structure	P_s (nC/cm ²)	$\delta\epsilon$	$\Delta\epsilon$	Ref.
Phenyl ester FLC mixture (KU-1010)	83.2	+0.08	-2.2	This work
HOBACPC 	75.0	+0.09	-0.02	16
LC1 	500	+4.40	-3.8	16
CD11 	90.0	+4.75	-1.0	16


 Figure 11 Temperature dependence of the dielectric biaxiality $\delta\epsilon$ and tilt angle θ in the SmC* phase.

natural order parameter for tilting transition is the tilt itself, which below T_c increases as $\theta = \theta_0(T_c - T)^\beta$, where θ is a tilt angle, β a critical exponent that may be expected to vary between 0.5 (mean field value) and 0.25 (in a tri-critical like). If the material is chiral, the tilt angle is coupled to a local polarization P_s , which is proportional to the tilt in the limit of a small tilt as $P_s \propto \theta = \theta_0(T_c - T)^\beta$. The transverse component ϵ_\perp of the permittivity splits into two different tensor components, ϵ_1 and ϵ_2 at transition SmA*-SmC*. The difference, $\delta\epsilon = \epsilon_2 - \epsilon_1$, that increased with increasing tilt angle, becomes zero in the SmA* phase, and does not depend on the sign of tilt, hence the $\delta\epsilon$ is proportional to θ^2 : $\delta\epsilon \propto (T_c - T)^{2\beta}$. In other words, the critical exponent of the biaxiality in the SmC* phase is twice that of the tilt angle. As shown with the solid line in Fig. 11, we find that an exponent for $\delta\epsilon$ is larger by a factor of 2 than the exponent of the tilt angle, which are 0.27 and 0.54, respectively. This result fulfils very well the expectation of being equal to 2β .

3.3. Optical response time

The measured optical response time as a function of applied field and temperature is shown in Figs 12 and 13. The critical slowing down near the SmC*-SmA* transition is apparent. Also, it is seen that τ_{C^*} reasonably well obeys the relation of $\tau_{C^*} \propto E^{-1}$ in the SmC* phase and then gradually becomes independent of electric fields, as predicted when the Goldstone mode is replaced by


 Figure 12 Electro-optic response times as function of the temperature and applied electric field, respectively: (a) SmC* phase, \blacktriangle ; 26°C, \circ ; 35°C, \blacklozenge ; 52°C, (b) SmA* phase, \bullet ; 58.3°C.

 Figure 13 Electro-optic response times as function of the temperature and applied electric field for the N* phase (\blacksquare : 75°C, \circ : 78°C) and SmA* phase (\bullet : 64°C).

the soft mode in the SmA* phase. As shown in Fig. 13, at the low temperature part of the SmC* phase, the intervals of field dependence in response time decrease with increasing electric field. This is not surprising as several different factors, including dynamics, contribute to the total optical response. In Fig. 14, the response time τ_{N^*} as function of temperature and electric field is plotted in the N* and SmA* phases, respectively. The

measured value of τ_{N^*} is on the order of 10 μ s. Response times are almost independent of the applied field. It may be qualitatively understood by the simple relation of $\tau_{N^*} = \gamma_1 / K_1 t_0$, where K_1 is a elastic constant, t_0 an equilibrium twist of cholesteric and γ_1 rotational viscosity of the director n . This relation is derived from the equation of the balance of torque which governs the dynamics of the helix rotation. As expected, the response is faster at high temperature and high field strength.

4. Conclusion

Electro-optic and dielectric properties for phenyl ester FLC mixture were studied in detail. Dielectric relaxation spectroscopy was used to study the molecular dynamics and dipolar ordering. In the SmA* phase, this is accompanied by a sharp increase in the dielectric strength $\Delta\epsilon_s$ on approaching T_C . At such high frequency (2 MHz), $\Delta\epsilon$ is usually negative in the SmC* and SmA* phase. In the N* phase, at lower frequencies, $\Delta\epsilon$ has a weakly positive value. In the SmC* phase, $\delta\epsilon$ is positive and its maximum value is less than 0.1. In the present case, none of the constituent molecules of our mixture has this polar structure. Therefore $\delta\epsilon$ may be enhanced by attaching a strong polar group to one of the benzene rings directly connected with the alkyl chain.

The measured γ_θ is of an average value of 1 Nsec/m² in the SmC* phase. An Arrhenius plot of the rotational viscosity gives a linear behaviour from which the activation energy is estimated to be 1.4 eV. The values of γ_ψ have been compared with those determined by the dielectric method. The results are shown a good agreement between these two methods. Our mixture shows optical response times of about 50 μ s at room temperature and low electric field down to 2 μ s for high electric field close to the SmC*-SmA* phase transition. In the N* phase, the value of the optical response time is on the order of 10 μ s and almost independent of the applied field.

Acknowledgements

This work was performed as a G-7 project supported by the Ministry of Commerce, Industry and Energy (MO-CIE) and Ministry of Science and Technology (MOST).

References

1. R. B. MEYER, L. LIEBERT, L. STRZELESKI and P. KELLER, *J. Phys. Lett.* **36** (1975) L68.
2. N. A. CLARK and S. T. LAGERWALL, *Appl. Phys. Lett.* **36** (1980) 899.
3. A. D. L. CHANDAI, Y. OUCHI, H. TAKEZOE, A. FUKUDA, K. TERASHIMA, K. FURUKAWA and A. KISHI, *Jap. J. Appl. Phys.* **28** (1989) L1261.
4. C. DESTRADE, S. PAYAN, P. CLUZEAU and H. T. NGUYEN, *Liq. Cryst.* **17** (1994) 291.
5. J. S. PATEL and J. W. GOODBY, *Mol. Cryst. Liq. Cryst.* **114** (1987) 117.
6. G. DURAND and PH. MARTINOT-LAGARDE, *Ferroelectrics* **24** (1980) 89.
7. E. P. POZHIDAYE, L. M. BLINOV, L. A. BERESNEV and V. V. BELYAYEV, *Mol. Cryst. Liq. Cryst.* **124** (1985) 359.
8. XUE JIU-ZHI, M. A. HANDSCHY and N. A. CLARK, *Ferroelectrics* **73** (1987) 305.
9. I. DAHL, S. T. LAGERWALL and K. SKARP, *Phys. Rev. A* **36** (1987) 4380.
10. J. C. JONES, E. P. RAYNES, M. J. TOWLER and J. R. SAMPLE, *Mol. Cryst. Liq. Cryst.* **7** (1990) 91.
11. H. ORIHARA, K. NAKAMURA and Y. ISHIBASHI, *Ferroelectrics* **85** (1988) 143.
12. K. YOSHINO, T. UEMOTO and Y. INUISHI, *Jpn. J. Appl. Phys.* **16** (1977) 571.
13. A. LEVSITIK, B. ZEKS, I. LEVSYIK, R. BLINC and C. FILIPIC, *Mol. Cryst. Liq. Cryst. Lett.* **56** (1980) 145.
14. C. LEGRAND, N. ISAERT, J. HMINE, J. M. BUISINE, J. P. PAMEIX, H. T. NGUYEN and C. DESTRADE, *J. Phys. II France* **2** (1992) 1545.
15. K. SKARP and S. T. LAGERWALL, *Ferroelectrics* **84** (1988) 119.
16. F. GOUDA, K. SKARP and S. T. LAGERWALL, *ibid.* **113** (1991) 165.
17. M. BUIVYDAS, F. GOUDA, S. T. LAGERWALL, M. MATUSZCZYK and B. STEBLER, *ibid.* **166** (1995) 195.
18. T. P. RICKER, N. A. CLARK, G. S. SMITH, D. S. PARMAR, E. B. SIROTA and C. R. SAFINYA, *Phys. Rev. Lett.* **59** (1987) 2658.
19. F. GOUDA, S. T. LAGERWALL, M. MATUSZCZYK and B. STEBLER, *Liq. Cryst.* **17** (1994) 291.
20. F. GOUDA, W. KUCZYNSKI, S. T. LAGERWALL, M. MATUSZCZYK, T. MATUSZCZYK and K. SKARP, *Phys. Rev. A* **46** (1992) 951.

Received 20 May 1999

and accepted 20 March 2000